GEO Collisional Risk Assessment Based on Analysis of NASA-WISE Data and Modeling

Jeremy Murray Krezan[1], Samantha Howard[1], Phan D. Dao[1], Derek Surka[2]

[1]AFRL Space Vehicles Directorate,[2]Applied Technology Associates Incorporated

From December 2009 through 2011 the NASA Wide-Field Infrared Survey Explorer (WISE) gathered radiometrically exquisite measurements of debris in near Earth orbits, substantially augmenting the current catalog of known debris. The NASA-WISE GEO belt debris population adds potentially thousands previously uncataloged objects. This paper describes characterization of the NASA-WISE GEO belt orbital debris population in terms of location, epoch, and size. Previous studies of collisional rate in GEO invoke the presence of a large number of debris in the region, with characteristic sizes too small to track, i.e. not in the catalog, but large enough to cause significant damage and fragmentation in a collision. We use new information suggested by the analysis of NASA-WISE infrared measurements to propose an updated GEO belt debris population. Our population estimate is an improvement over previous population estimates because of the unique characteristics of the NASA-WISE, a multispectral infrared imager. Based on the revised population estimate, we estimate the total collisional rate in the GEO belt with the inclusion of projected uncatalogued debris and application of a conjunction assessment technique.

1. INTRODUCTION

If orbital debris were all trackable to a high order of fidelity, it would be straightforward to determine the orbital safety risk to each and every satellite in orbit. Unfortunately, high fidelity tracking of debris has proven elusive and thus with respect to debris, questions about *orbital safety* typically concern both the distribution of debris and the impact of debris[1-9]. In this paper we describe efforts to use data from the NASA Wide-Field Infrared Survey Explorer (WISE) to first create a debris catalog, then estimate the distribution of debris as a function of size and via simulations based on that unique catalog of debris perform a GEO belt collisional risk calculation. The NASA-WISE is an infrared (IR) instrument built and flown by NASA and their partners for the purposes of astronomical observations. In summary the instrument is a Mid-Wave/Long-Wave solid-Hydrogen cooled 40cm telescope. The instrument spectral bands are (3.4, 4.6, 12, and 22 μm). More details of the instrument, including pre-launch instrument sensitivity are documented in Reference [10] and references therein. In addition to the astronomical measurements gathered with the NASA-WISE payload, the instrument captured imagery that contained unresolved measurements of space debris. Specifically, the NASA-WISE instrument captured unresolved measurements of space debris in the GEO belt. The Air Force Research Lab created a debris catalog that includes over 2,000 measurements of previously un-cataloged, debris objects near the GEO belt. The NASA-WISE instrument was able to create such an extensive catalog of debris during the short time that it was mission capable because it was flown in a low-earth orbit, and thus did not suffer outages due to weather or daytime conditions, it was a sensitive instrument with the capability to observe small warm debris, and due to the multispectral infrared capabilities of NASA-WISE, inference of debris size can be made.

Although GEO belt collisional risk assessments have been performed in the past, many have been based solely on simulation and all, including this investigation, suffer insufficient observational data to make a comprehensive assessment of all debris greater than 10cm in characteristic size, much less down to 1cm in characteristic size. Albeit insufficient to make a complete assessment, the NASA-WISE debris catalog offers a glimpse of the GEO belt debris population even down to 1cm. With the NASA-WISE catalog and the characterization of the GEO belt debris population, which allows simulation of unobserved debris, a conjunction assessment using previously vetted techniques[13-14] is relatively straightforward, and supplies an updated description of the GEO belt collisional risk.

2. DEBRIS ESTIMATION

The NASA-WISE instrument is particularly useful for characterization of debris due to the ability of IR remote sensing techniques to infer cross-sectional size. Assuming that all of the measured light is radiantly emitted and that the spectral emittance of debris objects in aggregate follow a grey-body spectrum[11], the temperature and effective cross section of the debris is inferred by a least-square fit of spectral radiant emittance as measured in different wavebands. Although greybody emittance is presumed, if measurements in different wavebands are treated relative to each other, then the exact value of the greybody emittance is not necessary. The systematic and random errors associated with this technique have been investigated in Reference[11]. These assumptions are only valid when the

reflected radiance is minimized. For results in this paper, only the longest wavelength bands, 4.6, 12, and 22 μm data are used for debris cross-section, or size estimation.

Using the distribution of debris as a function of size, the investigated model for size dependent distributions of debris near the GEO belt expresses observed frequency, *M*, as a function of cross-sectional area or characteristic radius, *r*, assuming spherical debris. Motivated by distributions such as those shown in Fig. 1, and previously published distributions such as those in Ref. [2-4], it is expected that the small debris will be distributed as a power-law with scaling factor τ[3][4].

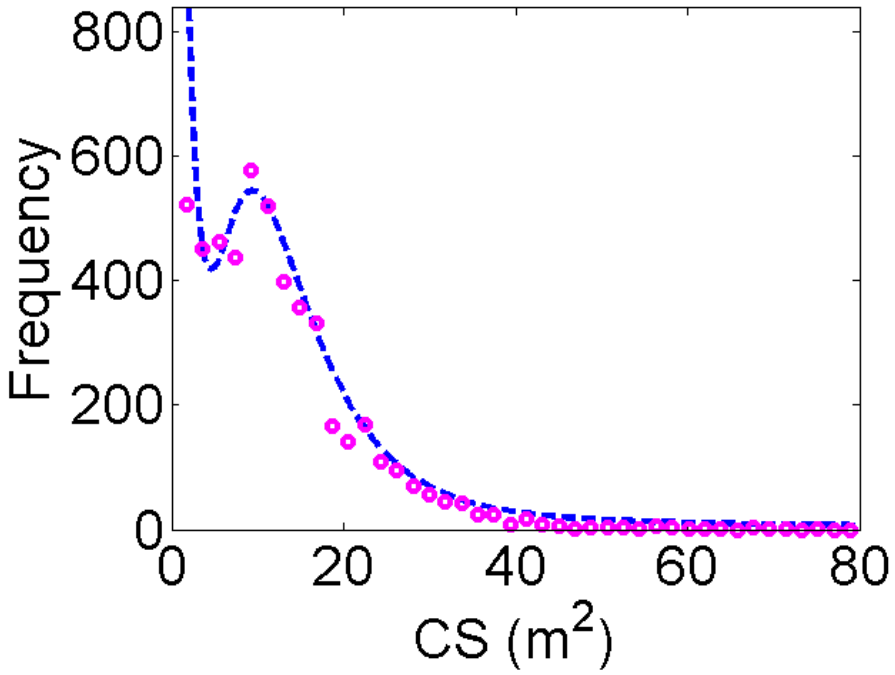

Fig. 1: Magenta Circles are NASA-WISE debris data distributed as a function of measured infrared cross-sectional (CS) area. The dashed blue line highlights a rough trend in the data.

Equation 1 shows a distribution function for small debris:

$$M(r) = B_1 f(r) r^{\frac{-5\ln(10)}{\tau}}, \qquad (1)$$

where *f(r)*is a function that describes the reduction of sensitivity due the NASA-WISE instrument. The sensitivity of the instrument, and a model for how that affects the distribution of NASA-WISE debris was reported on previously in Ref [12]. In that paper *f(r)* was described as a piece-wise function with maximum value of unity and beginning at a critical value $r=r_f$ a gradual roll-off to the minimum value of zero. Previously, we described τ as a characteristic length, in Eq. 1 τ is a scaling factor that, as *r* increases, represents how rapidly *M(r)* declines, from a maximum value near *r=0m*. Equation 1 is linearized by a log transform, where $y = log_{10}M$ and $x=log_{10}r$ is:

$$y = \begin{cases} a_1 x^2 + b_1 x + c_1, & x \le x_f \\ b_2 x + c_2, & x > x_f \end{cases}, \qquad (2)$$

where,

$$\log_{10} M^* = y = \begin{Bmatrix} y_1 \ , & \log_{10} r < \log_{10} r_f \\ y_2 \ , & \log_{10} r \geq \log_{10} r_f \end{Bmatrix} = \begin{Bmatrix} a_1 x^2 + b_1 x + c_1 \ , & x \leq x_f \\ b_2 x + c_2 \ , & x > x_f \end{Bmatrix}.$$

$$y_1 = \left[\log_{10} B_1 + \frac{\log_{10} e}{\tau} \left(5\log_{10} 37\text{e}6 - 26.74 + 2.5\log_{10} \frac{3\pi}{2} - \frac{25}{2\sigma_f^2} \left(\log_{10} r_f \right)^2 \right) \right]$$

$$+ \left[\left(\frac{-5}{\tau} + \frac{25}{\sigma_f^2} \log_{10} r_f \right) \log_{10} e \right] \log_{10} r + \left[\frac{25}{2\sigma_f^2} \log_{10} e \right] (\log_{10} r)^2.$$

$$\Rightarrow a_1 = \frac{-25}{2\sigma_f^2} \log_{10} e, \qquad b_1 = \left(\frac{-5}{\tau} + \frac{25}{\sigma_f^2} \log_{10} r_f \right) \log_{10} e.$$

$$\Rightarrow \sigma_f = \sqrt{\frac{-25}{2a_1} \log_{10} e}, \qquad \tau = \frac{-5\log_{10} e}{b_1 + 2a_1 \log_{10} r_f} = \frac{-5\log_{10} e}{b_2^*}.$$

$$c_1 = \log_{10} B_1 - b_2^* \left(\log_{10} 37\text{e}6 - 26.74/5 + 0.5\log_{10} 3\pi/2 + \frac{a_1}{5\log_{10} e} x_f^2 \right).$$

$$y_2 = \left[\log_{10} B_1 + \frac{\log_{10} e}{\tau} \left(5\log_{10} 37\text{e}6 - 26.74 + 2.5\log_{10} \frac{3\pi}{2} \right) \right] + \left[\frac{-5\log_{10} e}{\tau} \right] \log_{10} r = c_2 + b_2 x.$$

$$\Rightarrow b_2 = \frac{-5\log_{10} e}{\tau}, \qquad c_2 = \log_{10} B_1 - b_2 \left(\log_{10} 37\text{e}6 - 26.74/5 + 0.5\log_{10} 3\pi/2 \right). \tag{3}$$

$$\Rightarrow \tau = \frac{-5\log_{10} e}{b_2}, \qquad B_1 = 10^{c_2 + b_2 \left(\log_{10} 37\text{e}6 - 26.74/5 + 0.5\log_{10} 3\pi/2 \right)}.$$

Figure 2 shows a typical result for a piece-wise least squares fit to the NASA-WISE data. The circles show the data and lines show fitted distributions where $r_f = 0.37m$ and other parameters are described in Table 1.

Regression analysis assuming the form of Eq. 2 and a spline fit described in Ref.[12] gives the values of a_1,b_1,c_1,a_2, & b_2, or equivalently the values of τ, which physically represents the scaling parameter. Table 1 shows the least-squared fit results.

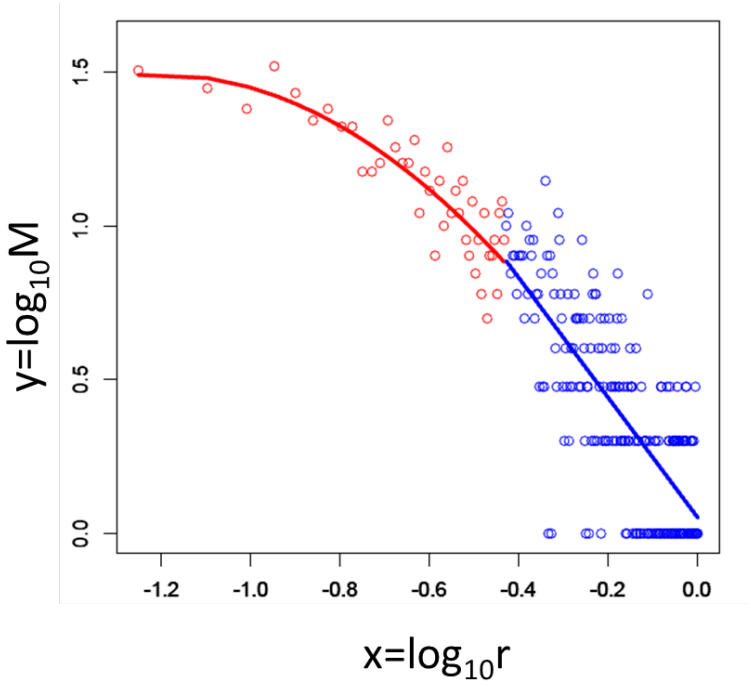

Fig 2: Split Fit, (circles) data and (lines) fitted distributions. Red color indicates data and fitted distributions where $x<xf$, blue indicates where $x>x_f$.

Table 1: Results of least square fit to NASA-WISE debris data.

r_f	a_1	b_1	c_1	b_2	c_2	τ_{approx}
0.361	-1.333	-3.002	-0.210	-1.974	0.052	1.15

Summation of the points under the curve in Fig. 2 yields an estimate of the total number of objects in the GEO belt. In order to understand the accuracy of this method, we analyzed the limited range of characteristic lengths *0.21>r>0.35m* or *-.68>x>-0.46*. The sum of the observations of GEO belt debris in that limited range is estimated to be 269, which is within 2.7% of the exact number countable in that range, 262 direct measurements. More generally we consider the accuracy of the approach when estimating the number of observations of GEO belt debris to be on the order of 5%. The total number of observations of GEO belt debris that the NASA-WISE instrument made is 2,461. This tally does not account for all of the debris that we estimate is missed due to the lack of sensitivity when the instrument observes small debris. However, we can use the regression analysis estimate of τ, to determine the value of Eq. 1 and approximate how many GEO belt objects would be observed under the assumption of perfect sensitivity. This estimate gives that with perfect sensitivity there would be 2,602 observations of objects greater than 10cm in characteristic length and 157,498 observations of objects with characteristic length greater than 1cm. Obviously the approximation of the number of objects greater than 1cm in characteristic length is a case of extrapolation, still there is reason to believe that the number of objects in the GEO belt, even down to 1cm in size would follow Eq. 1. The coverage of the NASA-WISE instrument was studied in detail, and cataloged debris were observed approximately 4.5 times per object during the limited time span of the NASA-WISE mission. With this estimate of coverage, the total count of observations gives us an upper limit on the number of GEO belt debris, with the lower limit estimated to be less by 4.5 times. Previously cataloged debris must be part of the total estimate as well and there are 458 debris objects in the NASA-WISE data set that are also in the public catalog. Using the described approximation, the total number of estimated debris with characteristic length greater than 10cm is between 1,036-3,060 and the total with characteristic length greater than 1cm is between 35,458-157,956.

3. DEBRIS SIMULATION

In the interest of calculating the GEO belt collision risk we use the estimated total debris population, the known cataloged objects in the GEO belt, and a rigorous application of a conjunction assessment algorithm. The debris measured by the NASA-WISE instrument, in addition to the debris assumed to exist based on the model for debris described in Sec. 2, approximate the total debris population and are used to generate two-line element sets (TLEs). In the case of the debris objects that are estimated to exist, but were not directly observed, the TLEs must be simulated. The conjunction assessment calculations based on the simulated TLEs and the catalog TLEs is performed with an algorithm and software application called the Continuous Anomalous Orbital Situation Discriminator (CAOSD). For these numerical experiments, CAOSD is deployed within the Advanced Research Collaboration and Application Development Environment (ARCADE), a Joint Space Operations Center (JSpOC) Mission System (JMS) test-bed, and provides a unique capability to compute the predicted conjunction flux between geostationary satellites and debris using the space catalog. The algorithm and software for CAOSD was developed to process all-on-all conjunction analysis for large numbers of objects (i.e. 100,000 or more) in a timely manner[13-14]. The basic algorithm for determining a conjunction includes propagation of orbits, associated uncertainty, and a combination of hardware and software innovations that enabled the original system to perform all-on-all conjunction analysis for the entire space catalog in less than 20 minutes[13]. The results have been validated in independent studies [14-15]. Subsequent enhancements and improved algorithms have reduced the processing time to less than 13 minutes, including special perturbations propagation [15]. Inputs to the CAOSD conjunction analysis are not limited to TLEs, but can include vector covariance messages (VCMs), or ephemerides. Given the few orbital elements determined from the NASA-WISE data— epoch, altitude (in km), inclination (in degrees), and right ascension of the ascending node (RAAN, in degrees)— the TLE format is the preferred option for simulated orbital debris. The inclination and RAAN map directly into TLEs, and altitude is converted to revolutions per day.

As already suggested, due to the limitations of the NASA-WISE observations, not all orbital elements could be derived. Therefore substitute values were determined, either from debris currently in the catalog or assumptions inherent in the object orbits. For example, the eccentricity is set to zero for all orbits due to an underlying assumption that the orbits are circular. This similarly leads to there being no perigee and thus the argument of perigee and the mean anomaly are undefined. A placeholder value of zero was supplied for both because they are CAOSD required inputs.

Other orbital elements not covered by the described assumptions or the mapped data are the first derivative of the mean motion with respect to time (divided by two), the second time derivative of the mean motion (divided by six, decimal assumed), and the BSTAR drag term (also called the radiation pressure coefficient). Consulting the satellite catalog on Space-Track.org, it is possible to sort by type and examine the debris objects only. In GEO orbit, there are 826 cataloged debris objects, including rocket bodies, which is a statistically large enough sample from which to determine typical characteristics. All had a second time derivative of the mean motion and BSTAR drag term equal to zero, allowing for the generalization of that value to all debris. The first derivative of the mean motion had a closely clustered distribution of values seen in Fig. 3, overlaid with a fit normal curve. In the interest of focusing variation amongst debris on those values measured by NASA-WISE, a single value of -0.00000120 was selected for use, falling between the mean of -0.00000116 and median of -0.00000124.

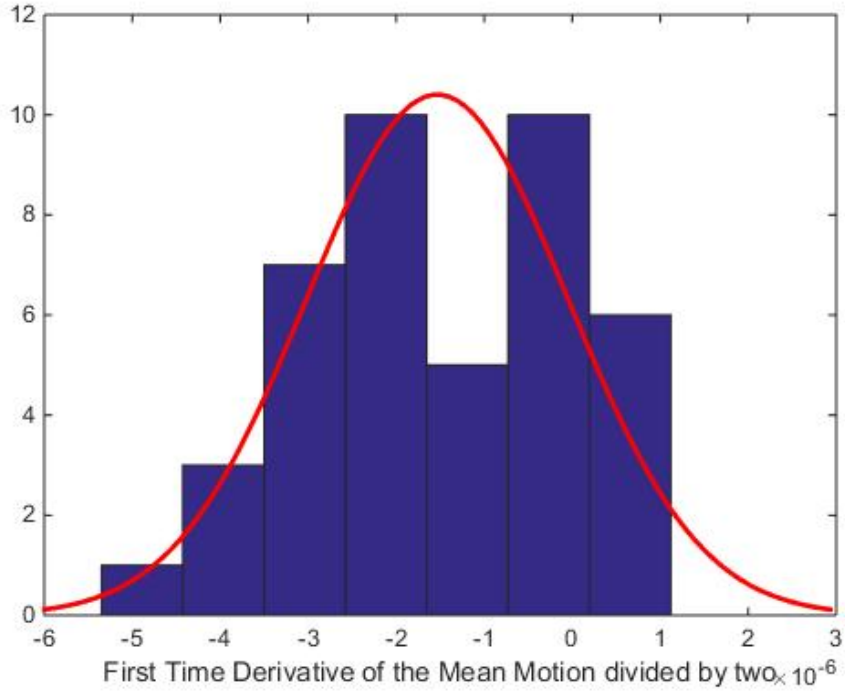

Figure 3: Distribution of the first time derivative of the mean motion divided by two for current debris objects in the catalog with a fitted normal curve (red line).

For the GEO belt debris objects that were not observed but rather are predicted to exist, the orbital parameters must be generated via simulations. Simulation of TLEs is performed by considering the distributions of the observed NASA-WISE debris and then generating random values for the TLE-set elements which conform to the distributions. Histograms fit with normal curves for altitude and inclination can be seen in Fig. 4. The mean and standard deviation were used as parameters for the built-in MATLAB random function. Also in Fig. 4 is the density of objects versus longitude: simulated TLE values representing the RAAN (correlated to longitude) were generated using a uniformly distributed random number.

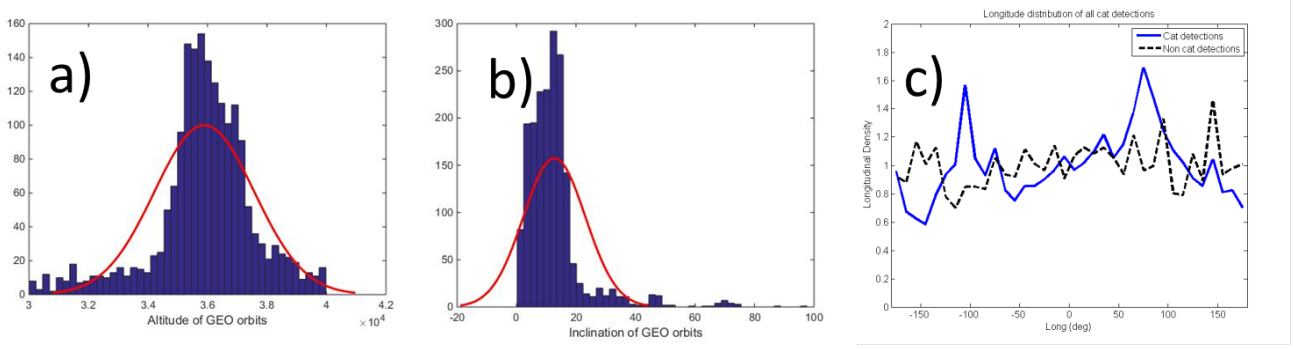

Figure 4: a) Altitude (km) distribution for NASA-WISE derived GEO debris with fitted normal curve (red line); b) Inclination (degrees) distribution for NASA-WISE-derived GEO debris with fitted normal curve (red line); c) Density as a function of longitude for NASA-WISE GEO belt debris and catalog objects.

4. RESULTS AND DISCUSSION

Simulated conjunctions were calculated as a function of different catalogs (2011 and 2015), for 1 and 5 simulated days, over variety of maximum conjunction distances. The results are both the *number of conjunctions* determined by the CAOSD algorithms and a derive *conjunction rate*. Plots of these results are shown in Figs. 5 and 6. The 2011 catalog is most comparable with the NASA-WISE debris data because that catalog was in use during the time of the NASA-WISE mission. The calculation with the 2011 and 2015 catalogs was performed to test if there was a difference due to the passage of time between 2011 and 2015.

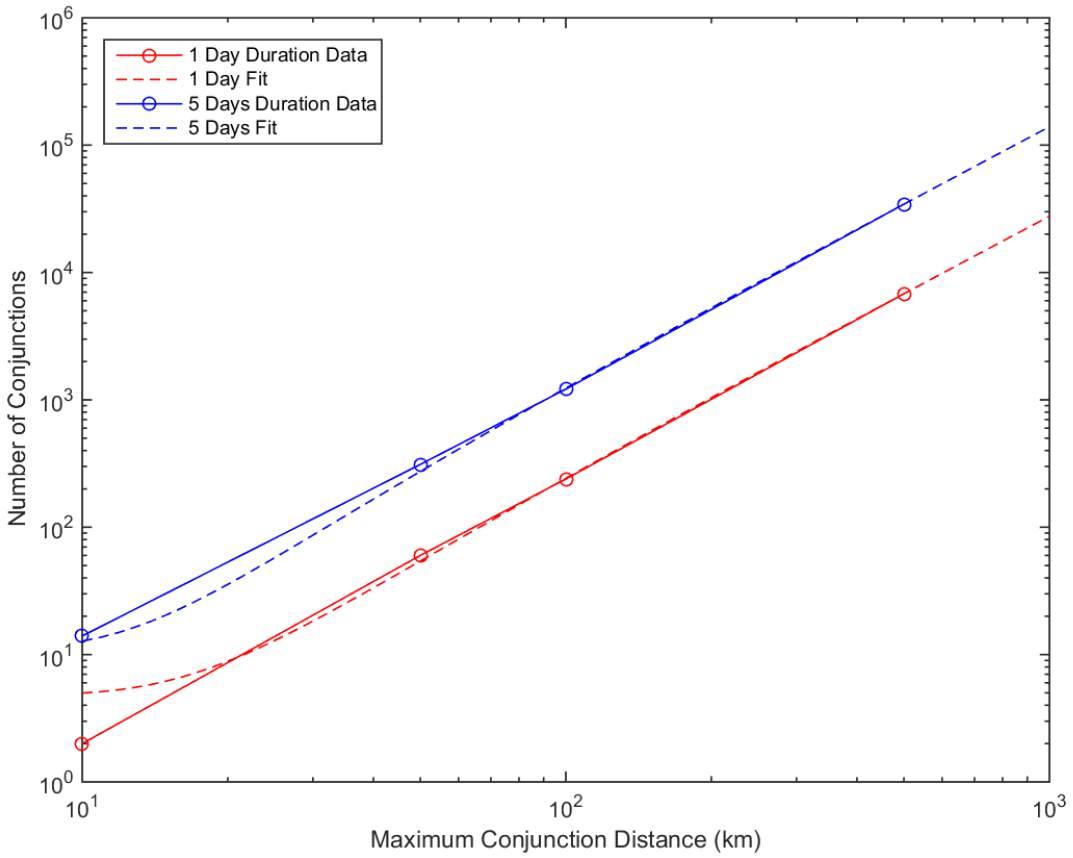

Figure 5: Number of conjunctions of the 2011 catalog with debris versus maximum conjunction distance in km for a one day time frame (red) and a five day time frame (blue)

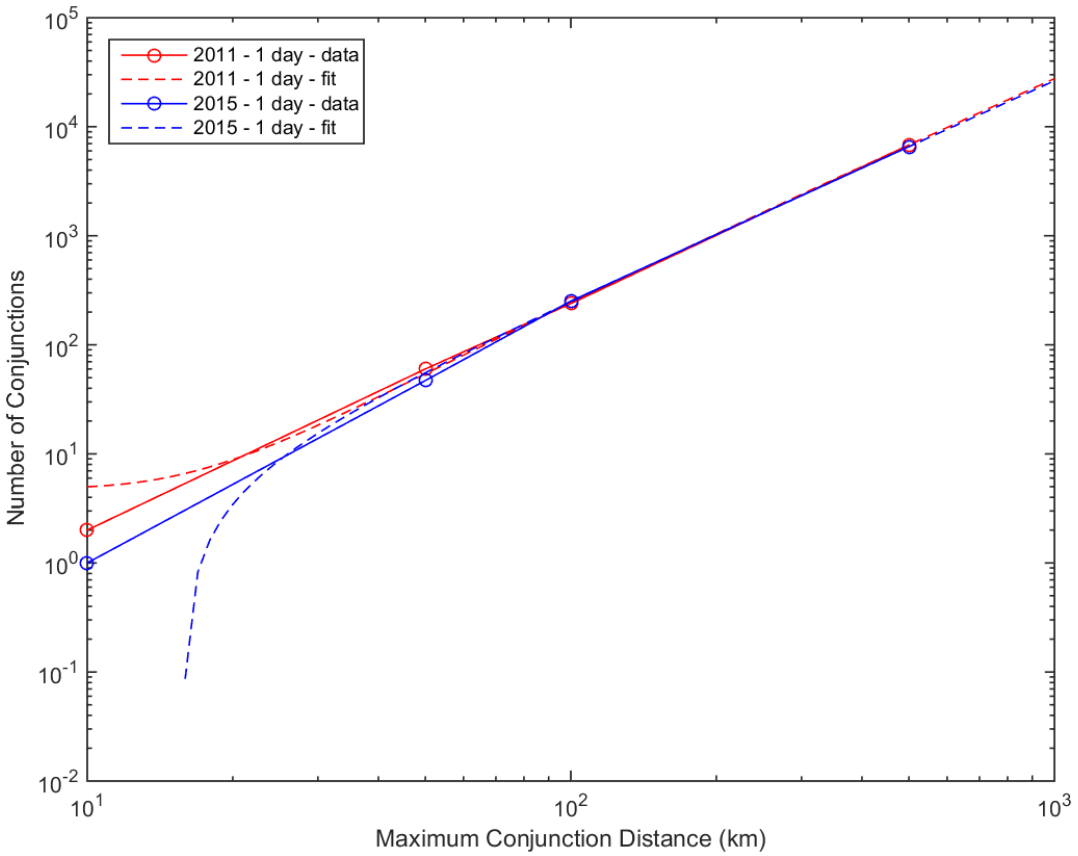

Figure 6: Number of conjunctions with debris versus maximum conjunction distance in km for a one day time frame against the 2011 catalog (red) and the 2015 catalog (blue)

In addition to calculation of the number of conjunctions, we use these results to estimate the conjunction rate. Following convention, we define the GEO collisional flux, f as the number of conjunctions for an object of 1 m^2 cross sectional area per year. Specifically to calculate the GEO collisional conjunction flux (conjunctions/m^2-yr) we use the following expression:

$$f_{GEO} = \frac{N_{D,\Delta t}}{\pi D^2 \Delta t} \qquad (6)$$

where D, or conjunction distance is determined from the CAOSD calculations and Δt is the duration of time for which conjunctions were assessed.

Table 2: Extrapolations from 2011 catalog results to conjunctions with debris per year per square meter

Time Frame	Lower bound	Estimate	Upper bound
1 day	2.88 x10^{-6}	3.26 x10^{-6}	3.64 x10^{-6}
5 days	3.18 x10^{-6}	3.28 x10^{-6}	3.38 x10^{-6}

Table 3: One day of conjunctions with debris per square kilometer

Catalog Year	Lower bound	Estimate	Upper bound
2011 (2855 obj)	0.025	0.028	0.031
2015 (3000 obj)	0.021	0.027	0.031

Because the goodness of fit coefficient on conjunction distance squared for 3,000 generated objects in 2015 falls within the 95% confidence interval of the 2,855 "actual" objects in 2011, it is safe to assume the results are comparable. Additionally, when the 2011 results are extrapolated out to the time frame of a year, the one and five day coefficients are also well within the 95% confidence interval of each other. Therefore, the results are consistent across actual and simulated data. Since the data from the 5 day time frame has a much smaller confidence interval, the associated fit will be used as the basis of further analysis.

Based on the curve fit in Fig. 6, it is estimated there are three conjunctions per day at a conjunction radius of 10km for the 3,000 generated objects of 10cm radius or larger. Table 4 shows how this value is expected to grow as the total population of GEO belt debris grows.

Table 4: Conjunctions with debris per day at a radius of 10km against the 2015 catalog. * indicates a value determined by a fit model rather than conjunction calculations.

Debris Objects	Conjunctions
3,000	3 *
35,000	32
87,500	76

The number of conjunctions increases nearly linearly with the number of debris objects, as is expected. Therefore the conjunction rate will similarly increase linearly.

The rate of conjunctions in GEO, based on 2,855 actual objects is estimated to be 3.281970 $x10^{-6}$/yr-m^2. Of course for a larger number of debris objects, the rate of conjunctions will increase, leading to the expected conjunction flux shown in Table 5. The last column of Table 5 shows the collisional probability, defined as the probability that there will be at least one collision per annum, is given by taking the results for the rates of conjunctions. The number of conjunctions is a function of the threshold distance according to,

$$N_2 = \left(\frac{D_2}{D_1} \right)^2 N_1 \qquad (7)$$

where the number of conjunctions N_1 corresponds with threshold distance D_1. Because determination of the number of conjunctions is stochastic, we must choose the values of threshold distance such that the number of conjunctions is statistically significant. As the number of conjunctions becomes significant, the collision flux asymptotically approaches a constant. The mean number of collisions c is approximated by

$$\begin{aligned} c_{GEO} &= f_{GEO}\ \overline{A}\ \Delta t \\ \overline{A} &= \pi\ \overline{d}^{\,2} \\ \overline{d} &= \sqrt{\frac{\sum_{k=1}^{K} (r_i + r_j)^2}{k}} \end{aligned} \qquad (8)$$

When the mean values are derived from all possible conjunctions in the catalog (SSN and NASA-WISE objects). Indices i and j span the entire catalog. Index k spans all possible pairs of catalog objects. The equivalent radius is approximated by the average of length, width, and height. Additionally, the equivalent radius may be approximated as the radius that results in a cross section equal to the SSN radar cross section. For objects not in the SSN catalog, the radius is related to the IR cross section.

Table 5: Extrapolated conjunctions with debris per day per square meter based on a linear-increase with number of debris objects

Debris Objects	Rate of Conjunctions	Annual Collisional Probability
2,855	3.28e-6	3.7e-3
35,000	3.83 $x10^{-5}$	1.3e-2
157,000	1.91 $x10^{-4}$	3.4e-1

As a sanity check the GEO belt collision probability per year for ~2,855 objects is on the same order as previous estimates for 1,000 debris objects (1e-3 collisional probability per year) presented in Ref. 9. Note that although the collisional probability values are on the same order, the direct calculation techniques using CAOSD in this work are more rigorous than the scaling arguments of those previous efforts.

The results described culminate in the GEO belt collisional risk for all cataloged objects versus all expected GEO belt debris. The unique contribution of this investigation, possible because of the NASA-WISE debris catalog is the direct identification of a few thousand new debris objects, and the estimate that there may be many thousand more debris objects near the GEO belt. The results of the collisional probability show that at the upper bound of the NASA-WISE debris limit there is a reasonably frightening chance of a collision every year, if the number of objects in the GEO belt is close to the upper limit predicted by the characteristics of the NASA-WISE debris catalog.

ACKNOWLEDGEMENTS

We are grateful to Kathleen Kramer, Don Mizuno, Tom Kuchar, and Emily Nystrom for their analysis to generate the AFRL NASA-WISE debris catalog, and to Air Force Research Lab leadership in the Space Vehicles Directorate, the Directed Energy Directorate, and the Summer Scholars Program for sponsorship of this work. And we owe a tremendous debt of gratitude to the NASA team who built, launched, and flew the WISE instrument and made that data available to AFRL.

REFERENCES

1. Klinkrad, H. *Space Debris: Models and Risk Analysis*, Praxis Publishing, Chichister, UK (2006).
2. Hanada, T. "Developing a Low-velocity Collision Model Based on the ANASA Standard Breakup Model," Space Debris 2.4 (2000): 233-247.
3. Liou, J.-C. "Orbital Debris Modeling," Presentation, 2012.
4. Schildknecht, T., et. Al. "Long-term Evolution of High Area-to-Mass Ratio Objects in Different Orbital Regimes," AMOS Technical Conference, Kihei HI, 2012.
5. Anderson, P.V., Schaub, H.,"Longitude-dependent effects of fragmentation events in the geosynchronous orbit regime", Acta Astronautica 105, 285-297 (2014).
6. Luu, K., Sabol, C., "Effects of perturbations on Space Debris in Supersynchronous Storage Orbits", Technical Report, Air Force Research Lab (1998).
7. Oltrogge, D., Finkleman, D., "Consequences of debris events in geosynchronous orbit", Proceedings of the 2008 AIAA/AAS Astrodynamics Specialist Conference and Exhibit, No. 2008-7375 (2008).
8. Chobotov, C. C. (Ed.), *Orbital Mechanics*, 3rd ed., American Institute of Aeronautics and Astronautics, Inc., Reston VA, 2002.
9. M. Hechler, "Collision Probabilities at Geosynchronous Altitudes', Adv. Space Rev. Vol. 5, No. 2, pp 47-57, 1985.
10. Larsen, M.F., "Wide-field Infrared Survey Explorer Science Payload Update", Proceedings of SPIE Vol. 7010 (2008); and references therein.
11. Paxson, C., Snell, H. E., Griffin, J. M., Kraemer, K., Price, S., Kendra, M., Mizuno, D., "Space Object Temperature Determination from Multi-Band Infrared Measurements," 2008 AMOS Technical Conference, Kihei, HI. September 2008.
12. Nystrom, E., Murray Krezan, J. "Distributions of Debris as Measured by the NASA-WISE Instrument," Proceedings of SPIE, Bellingham WA, (2015).
13. B. Abernathy, S. Harvey, D. M. Surka and M. O'Connor, "The CAOS-D Architecture for Conjunction Analysis," in *Infotech@Aerospace 2011 Conference*, St. Louis, 2011.

14. E. George and S. Harvey, "A Comparison of Satellite Conjunction Analysis Screening Tools," in *Proceedings of the Advanced Maui Optical and Space Surveillance Technologies Conference*, Wailea, 2011.

15. I. Budianto-Ho, C. Alberty, R. Scarberry, S. Johnson, and R. Sivilli, “Scalable Conjunction Processing using Spatiotemporally Indexed Ephemeris Data”, in *Proceedings of the Advanced Maui Optical and Space Surveillance Technologies Conference*, Wailea, 2014.